Electronic Supplementary Material (ESI) for Physical Chemistry Chemical Physics.

– Supplementary Information –

From high quality packing to disordered nucleation or phase separation in donor/acceptor interfaces: ClAlPc-C_{60} on Au(111)

Esther Barrena,[a] Rogger Palacios-Rivera,[a] José I. Martínez[b] and Carmen Ocal [a]*

[a] *Institut de Ciència de Materials de Barcelona (ICMAB-CSIC), Campus UAB, Bellaterra, E-08193, Barcelona, Spain.*

[b.] *Dept. Nanostructures and Low-dimensional Materials, Institute of Material Science of Madrid (ICMM-CSIC), Campus UAM, C/Sor Juana Inés de la Cruz 3, E-28049 Madrid, Spain*

* *E-mail: cocal@icmab.es*

Contact potential difference measurements.

The contact potential difference, CPD or V_{CPD}, can be measured from the parabolic dependence of the electrostatic force with the applied bias via the frequency shift:

$$\Delta f = -\frac{f_0}{4k}\frac{\partial^2 C(z)}{\partial z^2}(Bias - V_{CPD})^2,$$

where f_0, k, z, C(z) and V_{CPD} are, respectively, the resonance frequency, spring constant, distance, capacitance and contact potential difference of the tip-sample system.

The contact potential difference value depends on the work function of the tip and sample as:

$$V_{CPD} = \frac{\phi_{tip} - \phi_{sample}}{-e}.$$

In principle, knowing ϕ_{tip}, ϕ_{sample} can be calculated, but if the sample surface has regions with different electronic properties, as the case presented here, the contact potential difference between them will provide the difference in the local work function between regions *independently of the material the tip is made of*:

$$\Delta\phi = \phi_B - \phi_A = e[V_{CPD}(B) - V_{CPD}(A)].$$

In the present work, to obtain $\Delta\phi$ we perform spectroscopic curves consisting in the direct measurement of $\Delta f(V)$ through measuring the frequency shift versus applied bias over differentiated surface locations (A or B). To perform these spectroscopic measurements, at each location the tip was lifted away from the STM set point position.

As shown in Figure S1 for the incomplete bilayer studied in this work, topography and frequency channels are measured simultaneously (Figure S1a-b) to localize the diverse regions (A= first layer, B= second layer) and perform locally the spectroscopic $\Delta f(V)$ measurements (Figure S1c).

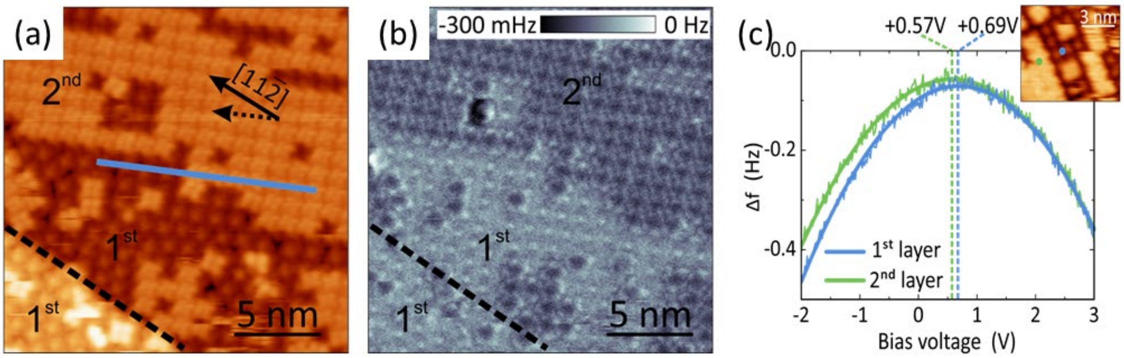

Figure S1. Topographic (a) and frequency shift (b) images of an incomplete ClAlPc bilayer. At the bottom left a substrate step can be identified under the molecular adlayer. First and second molecular layers and the substrate [112] direction are indicated. differentiated in the corresponding images by the color scale. The corresponding experimental CPD values for the two regions are extracted from the $\Delta f(V)$ curves in (c), corresponding to $\Delta\phi = 120\ meV$.

Substrate and ClAlPc adlayer models.

Before depositing C_{60} molecules, to construct all the ClAlPc/Au(111) trial system geometries used in the calculations (more than 20 have been checked) we have considered: i) a slab of four physical Au(111) layers with a minimum distance of ~ 25 Å of vacuum between neighbouring cells along the axis perpendicular to the surface, and ii) full periodic boundary conditions representing an infinite Au(111) surface. We have reproduced the unit cells experimentally obtained by keeping the evidenced molecular registry with the surface; with each substrate metal layer containing 30 Au atoms. After a full lattice optimization we obtained a unit cell of size (14.9×14.5) Å^2, each containing one and two ClAlPc molecules for the cases of one (Cl-up) and two (First layer: Cl-up, and Topmost layer: Cl-down) molecular layers, respectively. The theoretically obtained lattice parameters are slightly higher than the experimental values, mainly due to the unavoidable irreproducibility of the experimental Au(111) herringbone surface reconstruction within a theoretical periodic framework. For the structural optimization calculations only the two bottom Au(111) physical layers were kept fixed. The Brillouin zone was sampled for all the cases by means of a [2×2×1] Monkhorst-Pack grid, guaranteeing a full convergence in energy and electronic density.

Configurations choice of C_{60} on the ClAlPc/Au(111) adlayers: A large variety of configurational possibilities has been checked from a theoretical perspective. In order to that, different inequivalent adsorption sites have been analyzed for the interaction between the C_{60} molecules and each ClAlPc adlayer, namely the monolayer and the bilayer. For an appropriate selection of the different adsorption sites, two factors were considered: a) the location of the C_{60} molecules with respect to the Cl-up or Cl-down ClAlPc molecules forming the monolayer and the bilayer, respectively, and b) the orientation of the C_{60} molecules with respect to the ClAlPc molecules, which implies analyzing different "attacking" points of the C_{60} determining the interaction geometry between molecules.

Regarding the first factor for the case of Cl-up molecular monolayer, Figure 6 in the main manuscript shows C_{60} molecules located on three different adsorption sites: C_{60} molecules "on-top" of a Cl atom of the ClAlPc molecules, C_{60} molecules lying on a "molecular wing", and C_{60} molecules lying "on the hollow" between two "molecular wings" of two adjacent ClAlPc molecules.

Regarding the second factor, the C_{60} molecules have been considered to "attack" de Cl atom of the Cl-up molecules with a terminating C-atom, with a terminating C—C bridge (C_2-bridge in the text), and with a terminating C_6-ring (see Fig. 6). The resulting possible combinations of both factors would yield nine possibilities; nonetheless, the structural relaxation of the C_{60} molecules "attacking" by a terminating C-atom always led to relaxed structures with a terminating C_2-bridge or with a terminating C_6-ring, which reduces the possibilities from nine to six, just the panels shown in Fig. 6. Details in Figure S2.

A similar analysis of adsorption sites was considered to study the interaction of the C_{60} molecules with the topmost Cl-down molecular adlayer of the bilayer. In this case, we have considered two adsorption sites: C_{60} molecules on the center of a Cl-down molecule, and on a "hollow" left between two adjacent molecules of topmost molecular layer. Figure 7 shows the 4 different adsorption sites studied (2 with the interacting lowest part of the C_{60} being a C_6-ring and 2 with a C_2-bridge), and their corresponding optimized geometries. In this case, the most stable configurations are those with the C_{60} molecule lying on the Al atom of the Cl-down ClAlPc molecules with a bottommost C_2-bridge (Figure 7a) and a C_6-ring (Figure 7b). In consonance with the previous case, relaxation of configurations with a terminating C-atom of the C_{60} molecule led to any of the other two configurations. Details in Figure S3 and S4.

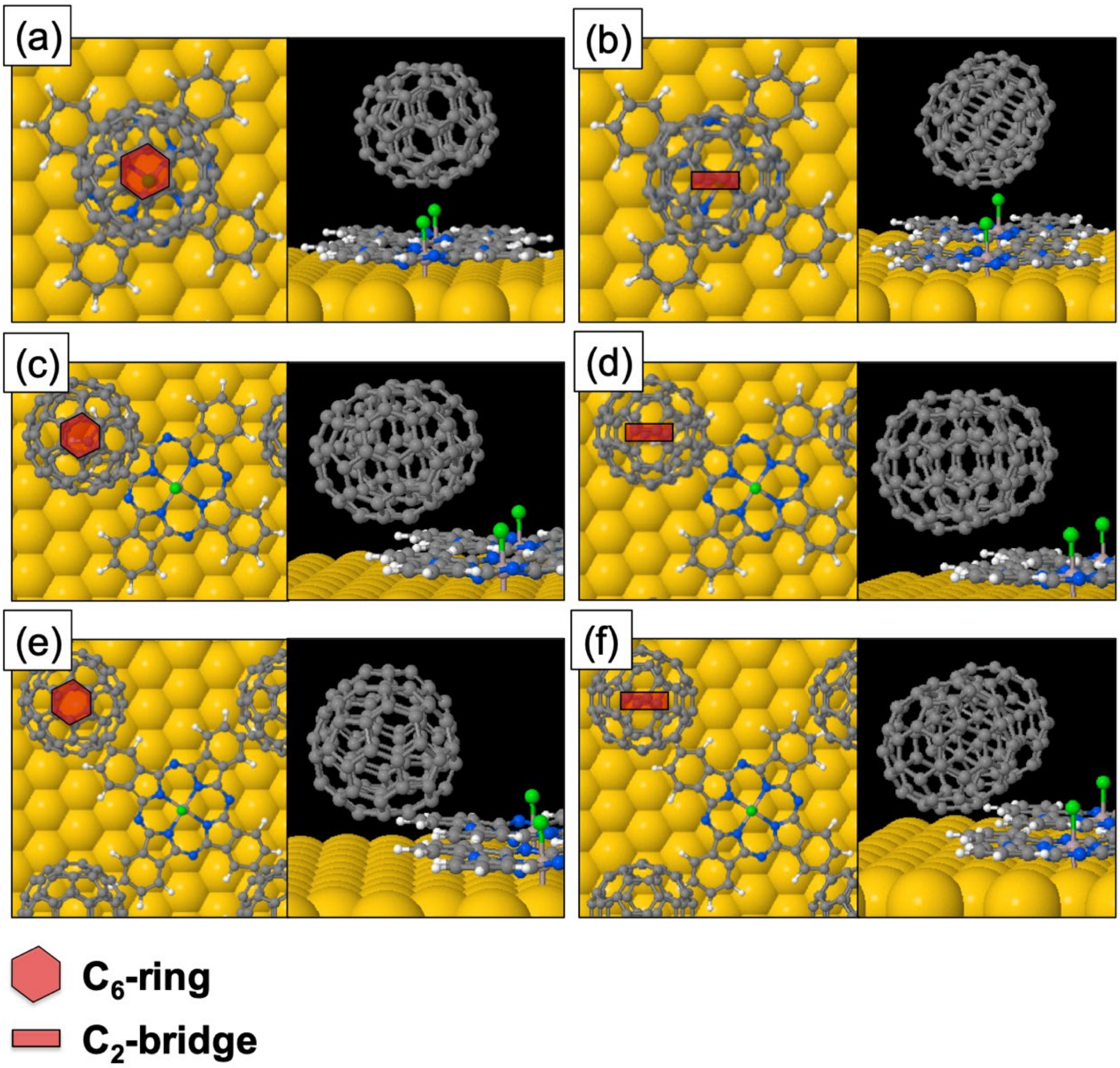

Figure S2. Zoomed panels of Figure 6 of the main text (top and side). Terminal C_6-rings and C_2-bridges are represented by red hexagons and rectangles, respectively.

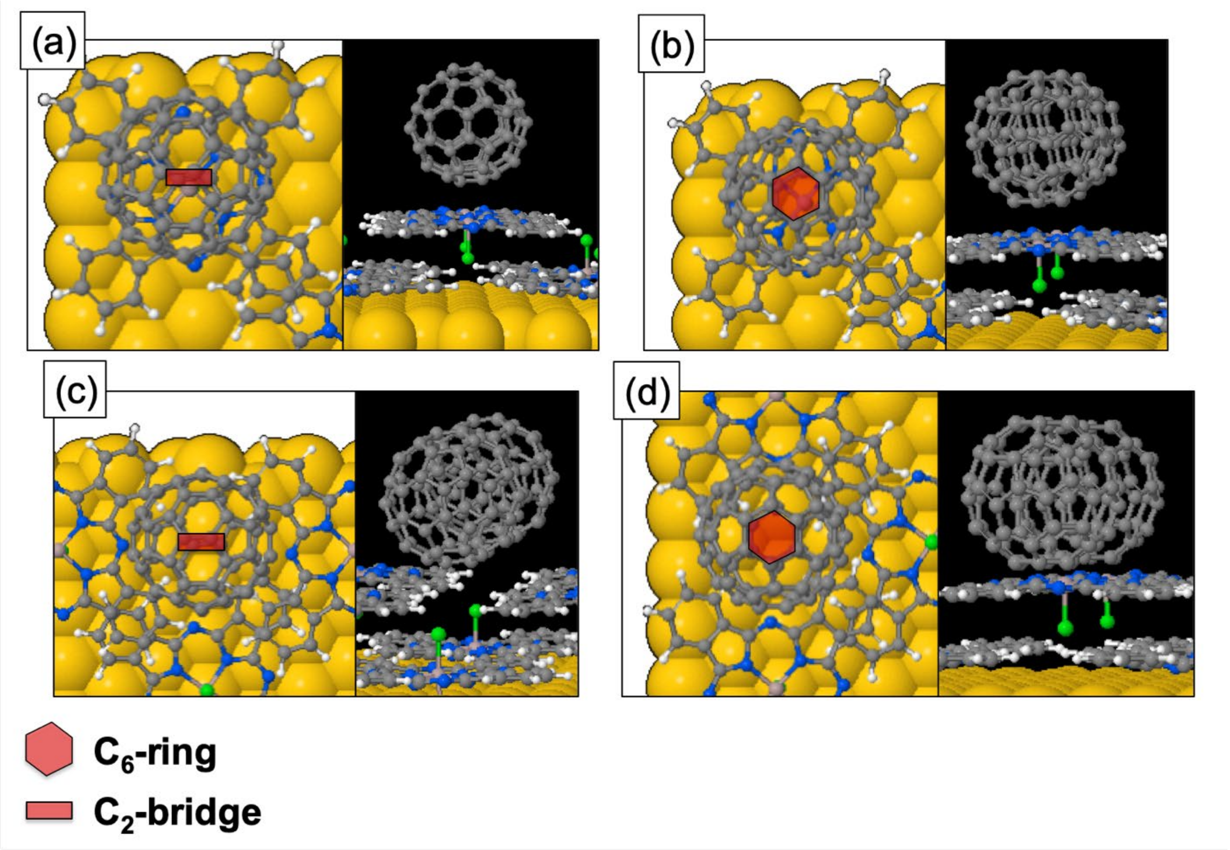

Figure S3. Zoomed panels of Figure 7 of the main text (top and side). Terminal C_6-rings and C_2-bridges are represented by red hexagons and rectangles, respectively.

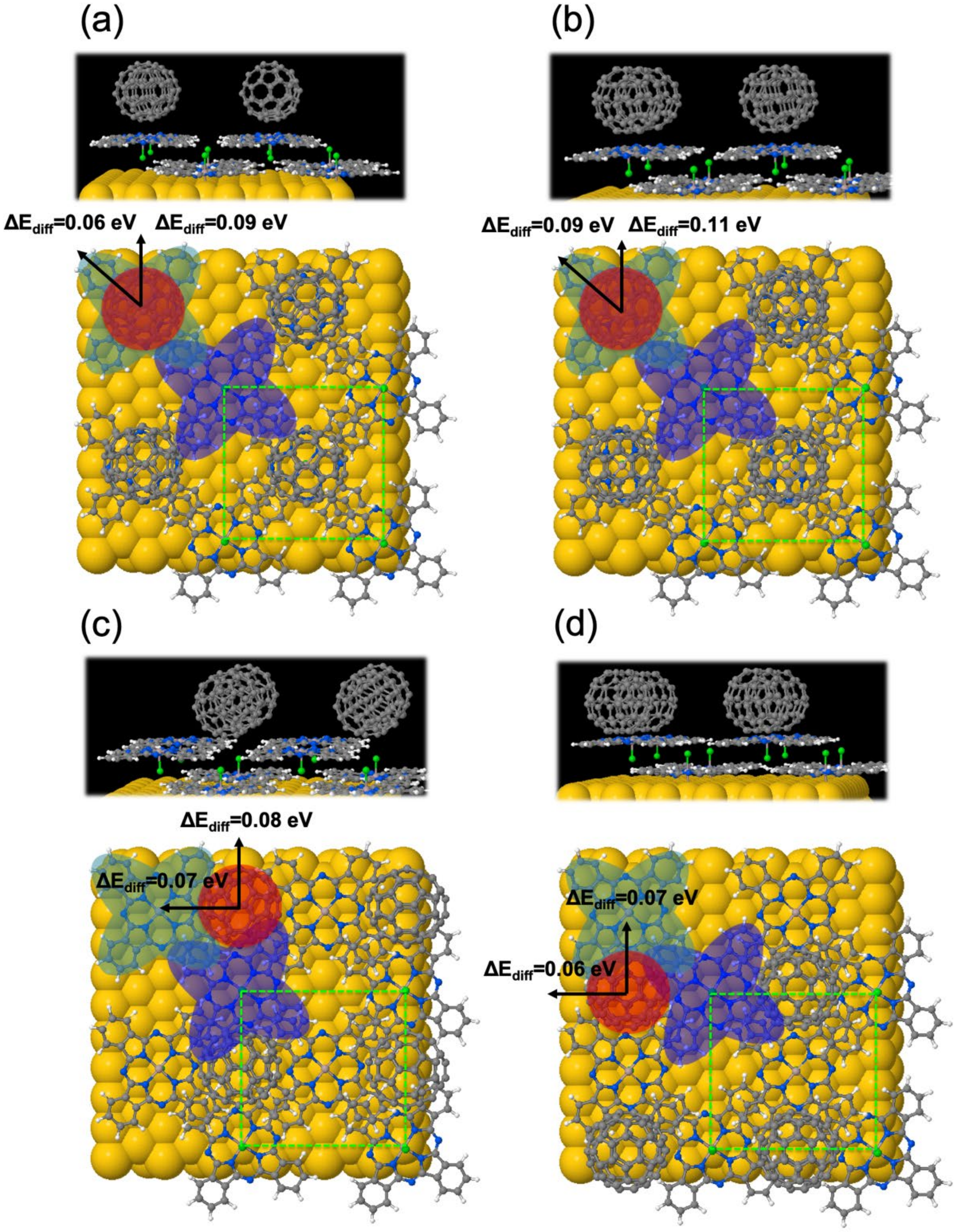

Figure S4. Top and side views of the DFT-optimized structural models for the adsorption of C_{60} on an ordered bilayer of Cl-up (bottom layer) and Cl-down (top layer) ClAlPc on Au(111). The unit cell used in the calculations is shown as a light-green dashed-lined box. Blue, green and red shadowed regions represent the Cl-up ClAlPc, Cl-down ClAlPc and C_{60} molecules, respectively. Computed CI-NEB diffusion barriers (ΔE_{diff}; in eV) are indicated along specified directions (black arrows) for each case.

Configurations in the gas-phase: The configurations considered for the interaction geometry in the gas-phase that are used in the main manuscript discussion to compare with those on the surface are shown in Figure S5. The two interaction energies for the configuration I (1.12 and 0.81 eV) correspond to interaction geometries of C_{60} facing the Cl atom with the C_2-bridge and C_6-ring, respectively, and are compared to the values (1.31 eV and 1.14 eV) for C_{60} on the Cl-up monolayer. For C_{60} facing the basal plane of ClAlPc (configuration II) we obtain considerably smaller interaction energies (0.36 and 0.32 eV) with C_2-bridge and C_6-ring, respectively, and almost null charge transfer (< 0.01 e-). These last gas-phase values are comparable to the adsorption energies of 0.48 and 0.56 eV given for each C_{60} configuration on the bilayer (topmost Cl-down layer). These results reinforce the three experimental evidences: i) lack of C_{60} adsorption on the Cl-down bilayer, ii) lack of ClAlPc adsorption on the C_{60} overlayer and iii) most stable C_{60} adsorption on the Cl-up ClAlPc monolayer on Au(111).

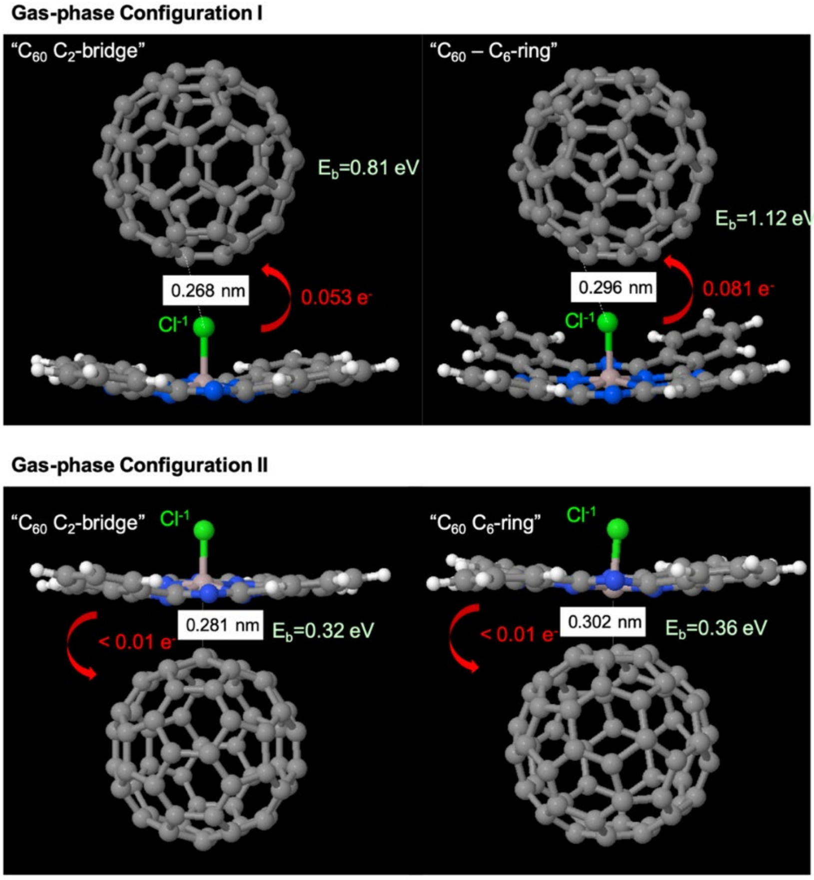
Gas-phase Configuration I

Gas-phase Configuration II

Figure S5. Two configurations for the interaction in gas-phase of a C_{60} molecule with a ClAlPc molecule. Configuration I with the C_{60} interacting with the Cl atom of the ClAlPc molecule, and Configuration II with the C_{60} interacting with the basal plane of the ClAlPc molecule. Both configurations analyzed for the C_{60} interacting through a C_6-ring or a C_2-bridge. Representative interaction distances, interaction energies and charge transfers are indicated for each case.